Control of Generator- and Grid-side Converter for the Interior Permanent Magnet Synchronous Generator

Tin Bariša, Damir Sumina, Martina Kutija
University of Zagreb, Faculty of Electrical Engineering and Computing
Unska 3, 10000 Zagreb, Croatia
tin.barisa@fer.hr, damir.sumina@fer.hr, martina.kutija@fer.hr

***Abstract*—Permanent magnet synchronous generators have wide application in wind energy conversion systems. If interior permanent magnet synchronous generator (IPMSG) is connected to the grid by a full scale AC-DC-AC converter, the wind turbine can be operated to extract maximum wind power at different wind speeds by optimally adjusting shaft speed. In this paper the model of the AC-DC-AC converter and related control structures for the control of IPMSG were developed in MATLAB/Simulink. Control of generator-side converter was achieved using field oriented control (FOC) which separately controls the electromagnetic torque and the magnetic flux. Optimal stator current references were calculated using maximum torque per ampere algorithm (MTPA) which ensures minimum stator current magnitude for electromagnetic torque reference. Control of grid-side converter was achieved using voltage oriented control (VOC) which separately controls active and reactive power injected to the grid. Outer control loop, with slower dynamics, ensures that DC circuit voltage is kept at reference value which ensures transfer of the active power from the DC circuit to the grid. Inner control loops, with faster dynamics, control the *d*- and the *q*-axis grid currents. Using developed control structures, the stator and the grid current PI controllers were designed using technical optimum while DC voltage PI controller was designed using symmetrical optimum. Proposed control methods were verified by simulation using laboratory model parameters.**

Keywords-AC-DC-AC converter; field oriented control; interior permanent magnet synchronous generator; voltage oriented control

I. INTRODUCTION

In recent years, wind energy conversion systems (WECS) have gained significant attention as clean and safe renewable power sources. Along with squirrel cage induction generators (SCIG) and double fed induction generators (DFIG), permanent magnet synchronous generators (PMSG) have wide application in WECSs [1]-[3].

Main characteristics of an interior permanent magnet synchronous generator (IPMSG) are high power factor, high power density, compact design, high efficiency and wide speed operating range. If IPMSG is connected to the grid by a full scale AC-DC-AC converter, the wind turbine can be operated to extract maximum wind power at different wind speeds by optimally adjusting shaft speed [4].

Generator-side converter control strategy aims to control separately magnetic flux and electromagnetic torque. This control strategy can be achieved by using direct torque control (DTC) or field oriented control (FOC). Main features of DTC are direct control of stator flux and electromagnetic torque, high stator current and torque ripple, excellent torque dynamics and variable switching frequency [5]. Field oriented control, often referred to as vector control, achieves stator current control using the synchronously rotating *dq* reference frame.

Grid-side converter control strategy aims to control independently active and reactive power transferred from the DC circuit to the grid. This control strategy can be achieved by using direct power control (DPC) or voltage oriented control (VOC). Main features of DPC are simplicity, fast dynamic response and variable switching frequency [5]. Voltage oriented control consists of outer control loop which keeps DC circuit voltage at reference value and inner control loops that control currents injected to the grid. The LCL grid filter is usually used to eliminate harmonics caused by pulse width modulation (PWM) of the grid-side converter [6].

In this paper the model of the AC-DC-AC converter and related control structures for the control of IPMSG were developed in MATLAB/Simulink. Control of the generator-side converter was achieved using field oriented control while control of the grid side-converter was achieved using voltage oriented control. Proposed control structures were used to design the stator and the grid current PI controllers using technical optimum and the DC circuit voltage PI controller using symmetrical optimum. Simulation was conducted using laboratory model data.

II. GENERATOR-SIDE CONVERTER CONTROL

A. Mathematical model of an IPMSG

The mathematical model of an IPMSG in synchronously rotating *dq* reference frame can be expressed as follows:

$$u_{sd} = R_s i_{sd} + L_d \frac{di_{sd}}{dt} - \omega_e L_q i_{sq} \tag{1}$$

$$u_{sq} = R_s i_{sq} + L_q \frac{di_{sq}}{dt} + \omega_e L_d i_{sd} + \psi_m \omega_e \tag{2}$$

$$T_e = \frac{3}{2} p \left(\psi_m i_{sq} + \left(L_d - L_q \right) i_{sd} i_{sq} \right) \tag{3}$$

where i_{sd} and i_{sq} are the *d*- and the *q*-axis stator currents, u_{sd} and u_{sq} are the *d*- and the *q*-axis stator voltages, T_e is the electromagnetic torque, ω_e is rotor angular electrical speed, R_s is the stator resistance, L_d and L_q are the *d*- and the *q*-axis inductances, ψ_m is the permanent magnet flux linkage, and p is

the number of pole pairs.

B. Field oriented control (FOC)

In Fig. 1 field oriented control structure of an IPMSG is shown. For given electromagnetic torque reference, optimal stator current references were calculated using maximum torque per ampere (MTPA) algorithm. Vector diagram of an IPMSG is shown in Fig. 2.

If stator currents in the *d*- and the *q*-axis are expressed depending on the stator current angle, the electromagnetic torque equation (3) can be written as follows [7]:

$$T_e = \frac{3}{2} p \left(-\psi_m I_s \cos\gamma + \frac{1}{2}\left(L_d - L_q\right) I_s^2 \sin 2\gamma \right) \tag{4}$$

where I_s is the stator current magnitude and γ is the stator current angle. According to MTPA algorithm, optimal stator currents in the *d*- and the *q*-axis ensure minimum stator current magnitude for given electromagnetic torque reference. Optimal stator current angle is found by calculating $\partial T_e / \partial \gamma = 0$:

$$\gamma = \arcsin \frac{-\psi_m + \sqrt{\psi_m^2 + 8 I_s^2 \left(L_q - L_d\right)^2}}{4\left(L_q - L_d\right) I_s} \tag{5}$$

Using (5) the optimal *d*-axis current can be expressed as a function of the *q*-axis current [7]:

$$i_{sd} = \frac{\psi_m}{2\left(L_q - L_d\right)} - \sqrt{\frac{\psi_m^2}{4\left(L_q - L_d\right)^2} + i_{sq}^2} \tag{6}$$

For the given electromagnetic torque reference, (6) is substituted into the electromagnetic torque equation (3) which leads to quadratic equation. Solution to that equation is the optimal *q*-axis stator current. After the optimal *q*-axis stator current is obtained, the optimal *d*-axis stator current is easily calculated using (3) or (6).

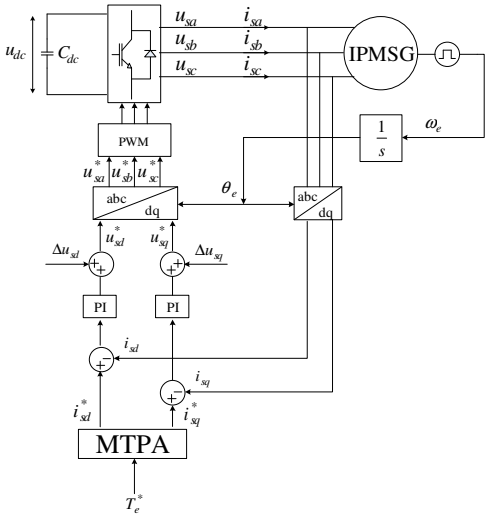

Figure 1. Field oriented control of an IPMSG

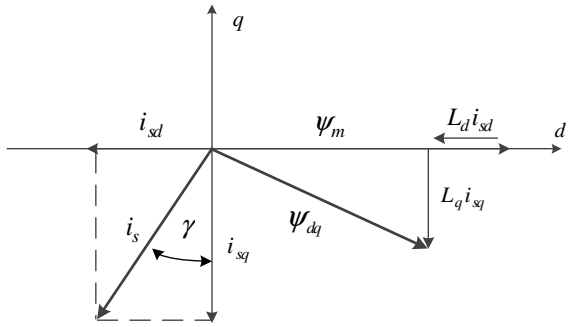

Figure 2. Vector diagram of an IPMSG

Calculated optimal stator current references are inputs to PI controllers. In order to achieve decoupled control in the *d*- and the *q*-axis, decoupling signals are added to outputs of PI controllers as follows:

$$\Delta u_{sd} = -\omega_e L_q i_{sq} \tag{7}$$

$$\Delta u_{sq} = \omega_e L_d i_{sd} + \psi_m \omega_e \tag{8}$$

where Δu_{sd} and Δu_{sq} are decoupling signals in the *d*- and the *q*-axis, respectively. Outputs of the PI controllers with decoupling signals form the *d*- and the *q*-axis generator-side converter voltage references. After inverse Clark and Park transformations, voltage references are forwarded to PWM.

C. PI controller design

Block diagram of the stator current control loop is shown in Fig. 3. Using decoupling signals (7)-(8) mathematical model of an IPMSG can be expressed as [8]:

$$u_{sd} - \Delta u_{sd} = i_{sd} R_s + L_d \frac{di_{sd}}{dt} \tag{9}$$

$$u_{sq} - \Delta u_{sq} = i_{sq} R_s + L_q \frac{di_{sq}}{dt} \tag{10}$$

Decoupled relations (9)-(10) are suitable for PI controller design. Gain and time constant of the IPMSG transfer function can be expressed as follows:

$$k_{d,q} = \frac{1}{R_s} \tag{11}$$

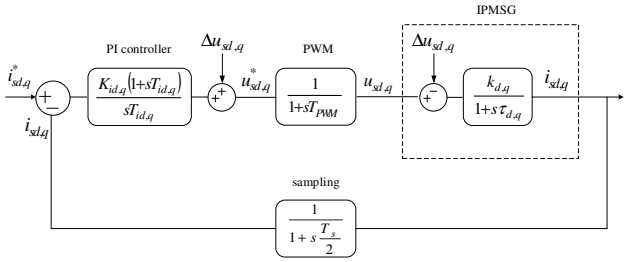

Figure 3. Block diagram of the stator current control loop

$$\tau_{d,q} = \frac{L_{d,q}}{R_s} \tag{12}$$

All measured values are sampled using sampling time T_s. Sampling and PWM are modelled as first-order elements with time constants T_{PWM} and $T_s/2$, respectively. To simplify the block diagram, two smallest time constants are grouped together as follows:

$$T_\Sigma = T_{PWM} + \frac{T_s}{2} \tag{13}$$

Since the IPMSG time constant is significantly bigger than the sum of PWM and sampling time constants, technical optimum is used for PI controller design. The dominant pole of the open loop transfer function can be cancelled by setting the integral time constant of the PI controller equal to the time constant of an IPMSG as follows [8]:

$$T_{id,q} = \tau_{d,q} \tag{14}$$

Gain of PI controller can be calculated as follows [8]:

$$K_{id,q} = \frac{1}{2}\frac{1}{k_{d,q}}\frac{\tau_{d,q}}{T_\Sigma} \tag{15}$$

III. CONTROL OF GRID-SIDE CONVERTER

A. Mathematical model of the LCL filter and the grid

Grid-side converter with LCL filter is shown in Fig. 4. Voltage equations between the grid-side converter and the grid can be expressed in stationary *abc* reference frame as follows [9]:

$$L_{1f}\frac{di_k}{dt} = u_k - i_k R_{1f} - u_{ck} \tag{16}$$

$$C_f \frac{du_{ck}}{dt} = i_k - i_{gk} \tag{17}$$

$$L_{2f}\frac{di_{gk}}{dt} = u_{ck} - i_{gk} R_{2f} - u_{gk} \tag{18}$$

$$k = a,b,c \tag{19}$$

where u_k is the grid-side converter voltage, i_k is the grid-side converter current, u_{ck} is voltage at the filter capacitor, i_{gk} is the grid current, u_{gk} is the grid voltage, L_{1f} and L_{2f} are filter inductances, R_{1f} and R_{2f} are filter parasitic resistances and C_f is the filter capacitor.

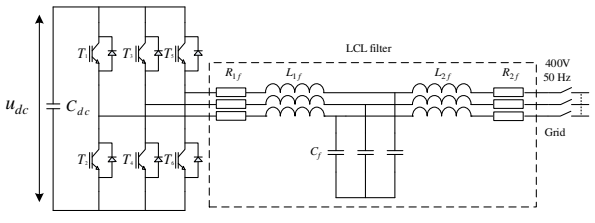

Figure 4. Grid-side converter with LCL filter

At frequencies that are lower than half of its resonance frequency, LCL filter can be modelled as L filter [9]. Resistance and inductance of the simplified model of the LCL filter can be expressed as:

$$R_f = R_{1f} + R_{2f} \tag{20}$$

$$L_f = L_{1f} + L_{2f} \tag{21}$$

where L_f and R_f are inductance and resistance of the equivalent L filter, respectively. Using simplified filter model and (16)-(19) voltage equations between the grid-side converter and the grid can be can be expressed in *dq* reference frame, which rotates with the grid voltage angular speed, as follows [9]:

$$L_f\frac{di_{gd}}{dt} = u_d - u_{gd} - R_f i_{gd} + \omega L_f i_{gq} \tag{22}$$

$$L_f\frac{di_{gq}}{dt} = u_q - u_{gq} - R_f i_{gq} - \omega L_f i_{gd} \tag{23}$$

where u_d and u_q are the *d*- and the *q*-axis grid-side converter voltages, u_{gd} and u_{gq} are the *d*- and the *q*-axis grid voltages, i_{gd} and i_{gq} are the *d*- and the *q*-axis grid currents, ω is the grid voltage angular speed, L_f and R_f are inductance and resistance of the filter, respectively.

B. Voltage oriented control

In Fig. 5 voltage oriented control of the grid-side converter is shown. Proposed control structure is achieved in *dq* reference frame which rotates with grid voltage angular frequency. In order to detect the grid voltage angle, phase locked loop (PLL) [10] is used. The *d*-axis of the *dq* reference frame is aligned with the grid voltage vector so the *d*-axis grid voltage is equal to its magnitude ($u_{gd} = u_g$) while the *q*-axis grid voltage is equal to zero ($u_{gq} = 0$).

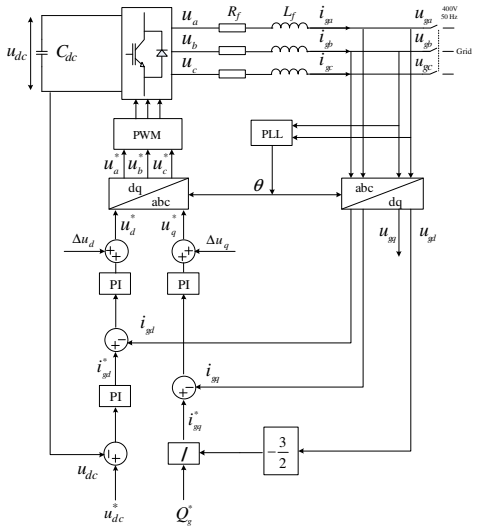

Figure 5. Voltage oriented control [11]

The outer DC voltage control loop keeps DC voltage at reference value which ensures that produced active power is transferred from the DC circuit to the grid. Output of the DC voltage PI controller is the *d*-axis grid current reference. The *q*-axis grid current reference can be calculated from the grid reactive power reference. Inner control loops, with faster dynamics, control the *d*- and the *q*-axis grid currents [11].

Calculated grid current references are inputs to PI controllers. In order to achieve decoupled control in the *d*- and the *q*-axis, decoupling signals are added to outputs of PI controllers as follows:

$$\Delta u_d = u_{gd} - \omega L_f i_{gq} \tag{24}$$

$$\Delta u_q = u_{gq} + \omega L_f i_{gd} \tag{25}$$

where Δu_d and Δu_q are decoupling signals in the *d*- and the *q*-axis, respectively. Outputs of the PI controllers with decoupling signals form the *d*- and the *q*-axis grid-side converter voltage references. After inverse Clark and Park transformations voltage references are forwarded to PWM.

C. PI controller design

Block diagram of the grid current control loop is shown in Fig. 6. Using decoupling signals (24)-(25) voltage equations between grid-side converter and the grid can be expressed as:

$$u_d - \Delta u_d = i_{gd} R_f + L_f \frac{di_{gd}}{dt} \tag{26}$$

$$u_q - \Delta u_q = i_{gq} R_f + L_f \frac{di_{gq}}{dt} \tag{27}$$

Decoupled relations (26)-(27) are suitable for PI controller design. Since the *d*- and the *q*-axis inductance are the same, gain and the time constant of the grid circuit transfer function are the same for both axis as follows:

$$k_i = \frac{1}{R_f} \tag{28}$$

$$\tau_i = \frac{L_f}{R_f} \tag{29}$$

Sampling and PWM are modelled as first-order elements with time constants T_{PWM} and $T_s/2$, respectively. Two smallest time constants are grouped as follows:

$$T_{\Sigma i} = T_{PWM} + \frac{T_s}{2} \tag{30}$$

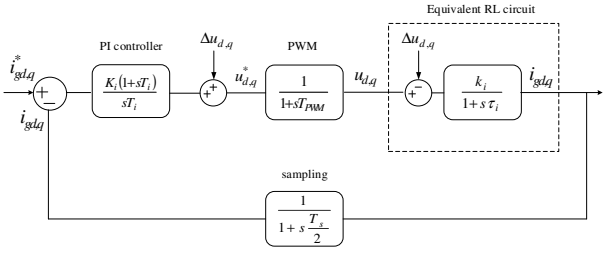

Figure 6. Block diagram of the grid current control loop

Time constant of the equivalent RL circuit between the grid-side converter and the grid is significantly bigger than sum of PWM and sampling time constants so technical optimum is suitable for PI controller design. Integral time of PI controller is used to cancel the dominant pole of the open loop transfer function as follows [12]:

$$T_i = \tau_i \tag{31}$$

Gain of PI controller is calculated as follows [12]:

$$K_i = \frac{1}{2}\frac{1}{k_i}\frac{\tau_i}{T_{\Sigma i}} \tag{32}$$

Simplified transfer function of the closed loop grid current control can be expressed as follows [12]:

$$G_{ci}(s) \approx \frac{1}{1 + 2T_{\Sigma i} s} \tag{33}$$

Block diagram of DC circuit voltage control loop is shown in Fig. 7. Active power of the DC circuit can be expressed as follows [8]:

$$P_{dc} = P_{gen} - P_g \tag{34}$$

$$C_{dc}\frac{du_{dc}}{dt}u_{dc} = P_{gen} - \frac{3}{2}u_{gd} i_{gd} \tag{35}$$

Linearization is performed around $u_{dc} = U_{dc}$, $u_{gd} = U_{gd}$, $P_g = P_{0,g}$, $P_{gen} = P_{0,gen}$. Linearized power balance equation, taking into account that generator and grid power are balanced in the steady state $P_{0,g} = P_{0,gen}$, can be expressed as [8]:

$$\Delta\frac{du_{dc}}{dt} = \frac{1}{U_{dc}C_{dc}}\Delta P_{gen} - \frac{1}{U_{dc}C_{dc}}\Delta P_g \tag{36}$$

Transfer function of the DC circuit voltage can be found using (36) as follows:

$$\frac{\Delta u_{dc}(s)}{\Delta P_g(s)} = -\frac{1}{sU_{dc}C_{dc}} \tag{37}$$

Grid current control loop is modelled using simplified expression (33) while sampling is modelled as first-order element with time constant $T_s/2$.

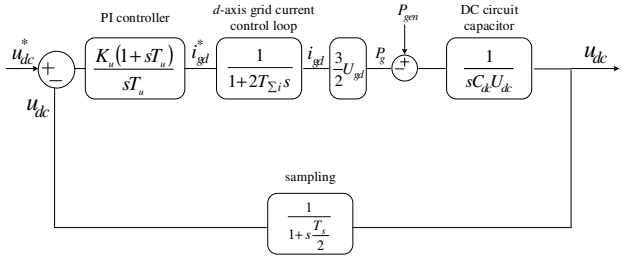

Figure 7. Block diagram of the DC voltage control loop

Open loop transfer function is obtained as follows [8]:

$$G_{ou}(s)=\frac{K_u\left(1+sT_u\right)}{sT_u}\frac{\frac{3}{2}U_{gd}}{1+2T_{\Sigma i}s}\frac{-1}{U_{dc}C_{dc}s} \tag{38}$$

Since the open loop transfer function includes integrator, symmetrical optimum is used for PI controller design. Two smallest time constants are grouped as follows:

$$T_{\Sigma u}=2T_{\Sigma i}+\frac{T_s}{2} \tag{39}$$

Gain and integral time constant of the PI controller can be expressed as follows [8]:

$$T_u=a^2T_{\Sigma u} \tag{40}$$

$$K_u=-\frac{1}{a}\frac{2}{3U_{gd}}\frac{U_{dc}C_{dc}}{T_{\Sigma u}} \tag{41}$$

where a is parameter related to the phase margin.

IV. SIMULATION RESULTS

The model of the AC-DC-AC converter and related control structures for the control of IPMSG were developed in MATLAB/Simulink as shown in Fig. 8. Parameters of the IPMSG are presented in Table I while parameters of the grid, AC-DC-AC converter and the LCL filter are presented in Table II. Given parameters were obtained from the laboratory model. Field oriented control described in Section II was used for the generator-side converter control. MTPA was used to calculate stator current references. Voltage oriented control described in Section III was used for the grid-side converter control. Technical and symmetrical optimums, described in Sections II and III, were used for PI controller design.

The electromagnetic torque reference was initially zero, it changed to -2389 Nm at 0.02 s and back to zero at 0.1 s. Reactive grid power reference was initially zero, it changed to 100 kVAr at 0.02 s and back to zero at 0.1 s. The electromagnetic torque, the DC voltage, the *d*-axis grid current, active grid power, mechanical power and reactive grid power are shown in Fig. 9. – Fig. 13.

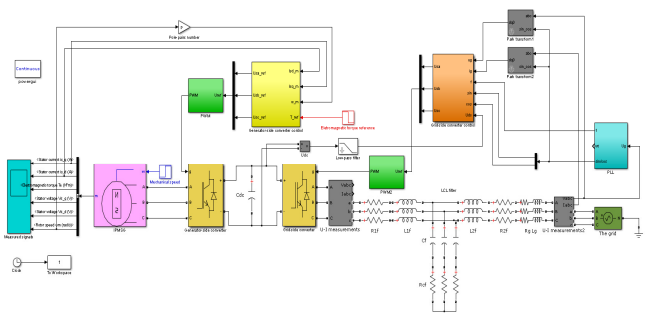

Figure 8. Simulink model of AC-DC-AC converter control

TABLE I. IPMSG PARAMETERS

Parameter	Value
Nominal power	P_n = 375 kW
Back EMF constant	266 V/krpm
Nominal current	I_n = 596 A
Nominal torque	T_n = 2389 Nm
Nominal frequency	f_n = 75 Hz
Nominal speed	n_n = 1500 rpm
Stator resistance	R_s = 8.05 mΩ
d-axis inductance	L_d = 0.72 mH
q-axis inductance	L_q = 1.06 mH
Permanent magnet flux linkage	ψ_m = 0.69 Wb

TABLE II. AC-DC-AC CONVERTER AND LCL FILTER PARAMETERS

Parameter	Value
Grid voltage	U_g = 400 V
Grid frequency	f_g = 50 Hz
DC circuit nominal voltage	U_{dc} = 750 V
DC circuit capacitance	C_{dc} = 11.76 mF
PWM switching frequency	f_{PWM} = 3 kHz
Filter capacitance	C_f = 136 μF
Converter-side filter inductance	L_{1f} = 45.61 μH
Grid-side filter inductance	L_{2f} = 31.85 μH
Converter-side filter parasitic resistance	R_{1f} = 0.12 mΩ
Grid-side filter parasitic resistance	R_{2f} = 1.97 mΩ

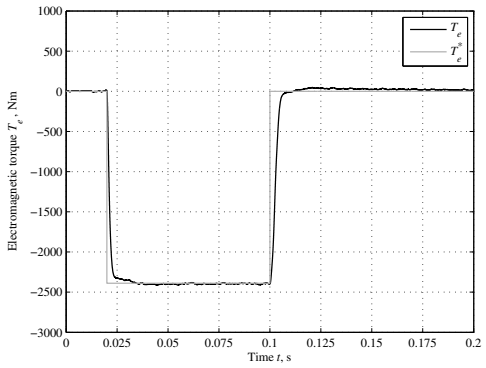

Figure 9. Electromagnetic torque

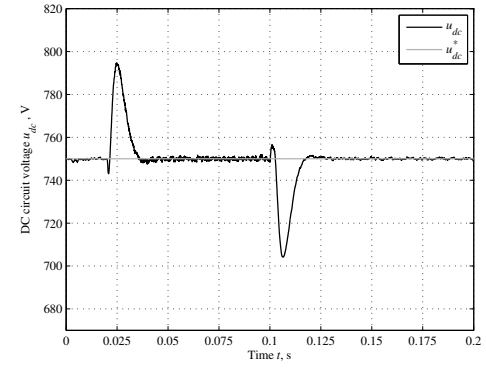

Figure 10. DC circuit voltage

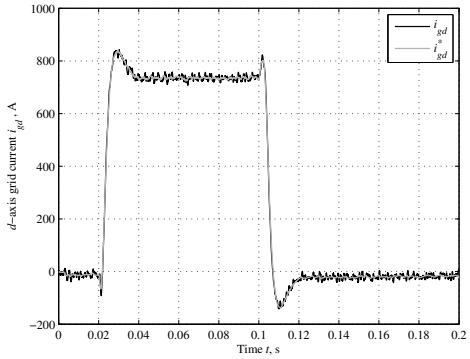

Figure 11. d-axis grid current

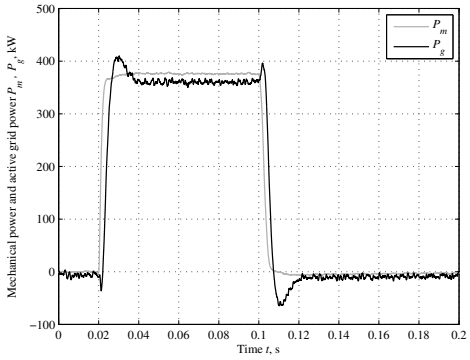

Figure 12. Mechanical power and active grid power

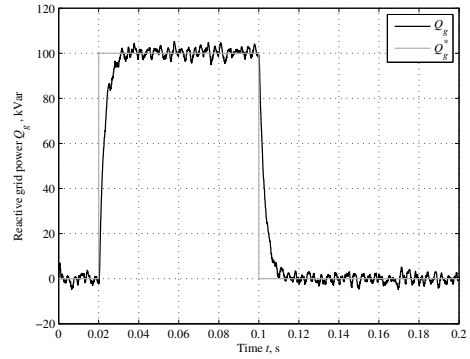

Figure 13. Reactive grid power

At 0.02 s active power was transferred from the IPMSG to the DC circuit which caused DC circuit voltage to rise. DC circuit voltage PI controller set the d-axis grid current reference to 730 A which ensured transfer of the active power from the DC circuit to the grid and restoring DC circuit voltage to reference value. The q-axis grid current reference was calculated using the reactive grid power reference and grid voltage measurement. For the reactive grid power reference 100 kVAr and grid voltage 400 V, the q-axis grid current reference was -205 A. Active grid power is smaller than mechanical power since there are power losses in the IPMSG, AC-DC-AC converter and LCL filter. In the steady state, mechanical power was 375 kW while active grid power was 360 kW.

V. Conclusion

In this paper simulation model for the generator- and the grid side converter control of the IPMSG was developed in Matlab/Simulink. Parameters of the laboratory model were used in simulation. Developed simulation model was used to determine optimal parameters of PI controllers. The stator and the grid current PI controllers were designed using technical optimum while the DC circuit voltage PI controller was designed using symmetrical optimum. Future work includes implementation of field oriented control for the generator side converter and voltage oriented control for the grid side converter. The proposed algorithms will be implemented on the digital control system based on ADSP-21992. Implemented algorithms will be verified on the laboratory model which consists of IPMSG, AC-DC-AC converter and induction motor which emulates wind turbine.

Acknowledgment

This work has been fully supported by the Croatian Science Foundation under the project number UIP-2013-11-7601.

References

[1] M. Chinchilla, S. Arnaltes, J.C. Burgos, “Control of permanent-magnet generators applied to variable-speed wind-energy systems connected to the grid,” *IEEE Trans. on Energy Conversion*, vol. 21, no. 1, pp. 130-135, Mar. 2006

[2] S. Morimoto, H. Nakayama, M.Sanada, Y. Takeda, “Sensorless output maximization control for variable-speed wind generation system using IPMSG,” *IEEE Trans. Ind. Appl.,* vol. 41, no. 1, pp. 60-67, Jan./Feb. 2005.

[3] S. Brabic, N. Celanovic, V. A. Katic, “Permanent magnet synchronous generator for wind turbine application,” *IEEE Trans. Power Electron.*, vol. 13, no. 3, pp. 1136–1142, May 2008.

[4] W. Qiao, L. Qu, R.G. Harley, “Control of IPM synchronous generator for maximum wind power generation considering magnetic saturation,” *IEEE Trans. Ind. Appl.,* vol. 45, no. 3, pp. 1095-1105, May/June 2009.

[5] N. Freire, “Fault-tolerant permanent magnet synchronous generator drives for wind turbine applications”, Ph.D. dissertation, Dept. Elect. Eng., Coimbra Univ., Coimbra, Portugal 2013.

[6] J. Dannehl, F. Fuchs, P.Thogersen, “PI state space current control of grid-connected PWM converters with LCL filters”, *IEEE Trans. Power Electron.*, vol. 25, no. 9, pp. 2320-2330, Sept. 2010

[7] G. Kang, J. Lim, K. Nam, H.B. Ihm, H.-G. Kim, “A MTPA control scheme for an IPM synchronous motor considering magnet flux variation caused by temperature,” *APEC 2004* nineteenth annual *IEEE*, vol. 3, pp. 1617-1621, Feb. 2004.

[8] V. Lešić, “Fault-tolerant control of a wind turbine subject to generator electromechanical faults”, Ph.D. dissertation, Dept. Contr. Eng., Zagreb Univ., Zagreb, Croatia 2014

[9] T. Hadjina, M. Baotić, N. Perić, “Control of the grid side converter in a wind turbine”, MIPRO 2013, pp. 925-930, May 2013

[10] V. Kaura, V. Blaško, “Operation of a phase locked loop system under distorted utility conditions”, *IEEE Trans. Ind. Electron.*, vol. 33, no. 1, pp. 58-63, Jan./Feb. 1997

[11] B. Wu, Y. Lang, N. Zargari, S. Kouro, “Control of grid connected inverter”, *Power Conversion and Control of Wind Energy Systems*, USA

[12] V. Blaško, V. Kaura, “New mathematical model and control of a three phase AC-DC voltage source converter”, *IEEE Trans. Power Electron.,* vol. 12, no. 1, pp. 116-123, Jan. 1997